This is a preprint, the final version is subject to change, of the American Mineralogist (MSA)
Cite as Authors (Year) Title. American Mineralogist, in press.
(DOI will not work until issue is live.) DOI: http://dx.doi.org/10.2138/am-2017-6017

1 **Revision 1**

2 Variations of Radon emanation coefficients as a function of physical and mineralogical
3 properties of a suite of naturally-occurring minerals

4 KATHERINE KRUPP, MARK BASKARAN*, SARAH J. BROWNLEE

5 Department of Geology, Wayne State University, Detroit, MI-48202

6

7 *: Corresponding author (Baskaran@wayne.edu)

8 American Mineralogist

9 Revised version

10 21 February 2017

11

12

13

14

15

16

17

18

This is a preprint, the final version is subject to change, of the American Mineralogist (MSA)
Cite as Authors (Year) Title. American Mineralogist, in press.
(DOI will not work until issue is live.) DOI: http://dx.doi.org/10.2138/am-2017-6017

Abstract

The escape rates of radon gas from rocks and minerals are of great relevance to many branches of geoscience and it is thus important to understand the physical and mineralogical properties that control radon emanation rates. Mechanisms of radon loss from minerals have direct bearing on the reliability of U-Pb and U-Th-He geochronology. Fourteen minerals from three different mineral groups and with localities spanning three continents were selected for this study. The radon emanation coefficients (REC) for each mineral were measured as a function of grain size, temperature, ^{238}U and ^{232}Th activities and total absorbed α-dose, density, and mineral melting temperature. The measured ^{238}U and ^{232}Th activities ranged from 0.01 to 6487 Bq g^{-1} and from below detection limit to 776 Bq g^{-1}, respectively. The REC values for unheated, pulverized samples ranged from 0.083 to 7.0%, which is comparable to previously reported ranges (except for zircon). An inverse correlation between grain size and REC was observed. Full annealing of fission tracks resulted in an overall decrease in REC values, suggesting that nuclear tracks could possibly act as conduits for radon release. While activity, alpha dose, density, and melting temperatures are not strongly correlated with REC values, it was observed that minerals with high melting points (≥1400°C) have lower REC values, most likely due to inhibition of radon release by compact crystal-lattice structures. This is the first attempt, to our knowledge, to correlate REC values with melting temperature, and this study reports six minerals for which no REC values have been previously reported.

Keywords: Radon emanation, REC, metamict minerals, nuclear track annealing, uranium

This is a preprint, the final version is subject to change, of the American Mineralogist (MSA)
Cite as Authors (Year) Title. American Mineralogist, in press.
(DOI will not work until issue is live.) DOI: http://dx.doi.org/10.2138/am-2017-6017

INTRODUCTION

The studies of radon emanation rates from soils, rocks, and minerals have a wide range of applications in many branches of geosciences. The escape of radon from rocks and minerals is of importance to geological dating, where it can limit the reliability of U-Pb geochronology (e.g., Heaman and LeCheminant 2000; Corfu 2012; Goa et al. 2014). Radon concentration gradients observed in air (both interstitial soil and atmospheric air in planetary boundary layers and above) and groundwater are widely used as tracers in order to predict earthquakes, locate subsurface uranium ore and hydrocarbon deposits, and study atmospheric transport (Garver and Baskaran 2004; Nazaroff 1992; Levinson et al. 1982; Fleischer and Mogrocampero 1985; Wakita et al. 1991; Fleischer and Turner 1984; Tanner 1964, 1980; Liu et al. 1984; Kritz et al. 1993; Baskaran 2016). Radon is also used as a tracer for quantifying the rate of gas exchange across the air-sea interface (Broecker et al. 1967; Baskaran, 2016). Furthermore, the inhalation of radon and its progeny poses a radiation health hazard, as radon was classified as a human carcinogen (in the same carcinogen group as tobacco smoke, asbestos, and benzene) in 1988 by the International Commission on Radiation Protection (IARC; WHO, 2009). For these reasons, it is important to understand the physical and geological factors that affect radon release rates from rocks, minerals, and soils.

During the alpha decay of ^{226}Ra, both an α-particle with a range of ~10,000 nm in solids and an energetic ^{222}Rn recoil nucleus are produced. With a recoil energy of 85 keV and a recoil distance of ~40 nm (e.g., Amin and Rama 1986: 35 nm in clays, 95 nm in water and 64,000 nm in air), the recoil nucleus of ^{222}Rn can collide with other atoms in a mineral's crystal lattice structure and alter their arrangement (Semkow 1990). In minerals where the radiation dose exceeds ~10^{16} α-decay events mg^{-1}, the mineral is reported to undergo a

This is a preprint, the final version is subject to change, of the American Mineralogist (MSA)
Cite as Authors (Year) Title. American Mineralogist, in press.
(DOI will not work until issue is live.) DOI: http://dx.doi.org/10.2138/am-2017-6017

radiation-induced transition from the crystalline to amorphous state (Murakami et al. 1991; Weber et al. 1994). The degree of internal radiation damage to the mineral structure by recoil and fission tracks can affect a mineral's radon emanation coefficient (REC, also known as coefficient of emanation, escape ratio, escape-to-production ratio, and percent emanation), which is the ratio of radon emitted to radon produced within the mineral. These nuclear tracks can become interconnected and increase the internal surface area of the mineral, promoting further escape of radon atoms. Radon atoms, upon formation from the decay of ^{226}Ra and located primarily within recoil distance, migrate either 1) from the edge of a mineral grain into pore space or pore water, 2) deeper into the mineral grain, 3) into an adjacent grain, or 4) into pore space by indirect or penetration recoil (Semkow 1991). The 40 nm recoil distance of radon atoms implies that only those ^{226}Ra atoms that lie extremely close to the surface (within 100 nm) can contribute directly to radon emanation. However, if there are large internal surface areas formed from weathering, corrosion from chemical reactions, or intensive fracturing on a microscopic scale, then, a fraction of radon atoms located within deeper regions of the mineral could undergo emanation from the grain. It is therefore important to study the escape of radon gas as a function of specific physical properties which could impact the extent of its recoil range and diffusion, including radiation damage, mineral density and melting point.

A large body of REC values of minerals and soils has been published. However, there are only a few naturally occurring minerals for which REC values are available. Of the 3000+ naturally-occurring minerals, it appears that REC values are available for less than 50 minerals (e.g. Turekian et al. 1977; Nazaroff 1992; Garver and Baskaran 2004; Sakoda et al. 2011; Malczewski and Dziurowicz 2015; Eakin et al. 2016). The purpose of this study is to

This is a preprint, the final version is subject to change, of the American Mineralogist (MSA)
Cite as Authors (Year) Title. American Mineralogist, in press.
(DOI will not work until issue is live.) DOI: http://dx.doi.org/10.2138/am-2017-6017

87 determine how the radon emanation rates of individual minerals are influenced by 1) grain
88 size, 2) nuclear track annealing, 3) ^{226}Ra concentration and alpha dose, and 4) melting point
89 and density. It is hypothesized that REC values should be inversely correlated to grain size,
90 should decrease with nuclear track annealing, alpha dose, and be inversely related with both
91 melting point and density. This is the first attempt, to our knowledge, to study the
92 relationship between radon emanation and melting temperatures of minerals. Furthermore,
93 this study includes six minerals that have never been used for REC studies and thus contains
94 their first reported REC values.

95 **MATERIALS AND METHODS**

96 Fourteen minerals from three different mineral groups (10 silicates, 3 oxides, and 1
97 phosphate) with localities spanning three different continents were selected for this study.
98 The location, specific gravity, geologic age, and chemical and mineralogical description of
99 all samples are given in Table 1. The specific gravity of the mineral samples ranged from
100 2.54 – 11.0 (silicates: 2.54 – 5.3; oxides: 4.3 – 11.0; phosphate: 2.9 – 3.5), and the melting
101 temperatures ranged from 1100 - 2827°C (silicates: 1100 -2200°C; oxides: 1356 - 2827°C;
102 phosphate: 1600°C). The estimated age of the mineral samples based on their source
103 formations ranged from 1050-1400 Ma, with the exception of two zircon samples from
104 different locations (Malawi, Africa zircon: 730 ± 20 Ma; Mud Tank, Australia zircon: 732 ±
105 5 Ma). A single large crystal of each of the mineral samples was crushed and sieved into
106 designated grain size fractions. To study radon emanation rate as a function of grain size,
107 three unheated zircon specimens from different localities were crushed and sieved into four
108 grain size fractions (<63, 63-125, 125-250, and 250-500 μm; these samples were prepared
109 and used in a previous study by Eakin et al. (2016)). In order to study radon emanation as a

This is a preprint, the final version is subject to change, of the American Mineralogist (MSA)
Cite as Authors (Year) Title. American Mineralogist, in press.
(DOI will not work until issue is live.) DOI: http://dx.doi.org/10.2138/am-2017-6017

function of nuclear track annealing, four minerals were tested in addition to the zircon samples from three localities, which were selected due to their relatively high concentration of uranium and thorium (Table 1). The 125-250 μm size fractions were heated to 25 (unheated), 200, 300, 400, 600, and 800°C for 6 hours. Seven additional minerals were chosen to represent a broad range of melting points and were pulverized to <125 μm.

Activities of ^{238}U and ^{232}Th

The activities of ^{238}U and ^{232}Th in the mineral grains were determined from the measurements of their progeny, ^{226}Ra and ^{228}Ra, respectively, using a high-purity germanium well detector coupled to a Canberra DSA-LX multi-channel analyzer, assuming secular equilibrium between the parents and their progeny. This ultra-low background Ge detector with ultra-low background hardware enabled us to measure very low ^{226}Ra activities (0.001 Bq g^{-1}, equal to 0.6 dpm in 10-g sample and with a dpm/cpm ratio of ~25, we get 40 counts with an error of 16%). Approximately 0.5 to 10 g of each size fraction, weighed to a precision of 0.1 mg, was placed in a 10 ml graduated counting vial. Radium-226 was measured using the 352 keV (^{214}Pb) and 609 keV (^{214}Bi) gamma energy peaks, ^{228}Ra was assayed using the 338 keV and 911 keV via ^{228}Ac gamma energy peaks, and both of their mean activities were calculated. The activity obtained by two different gamma-ray lines for both ^{226}Ra and ^{228}Ra agreed within 1σ. Typical resolution (full-width at half-maximum) was ~1.3 keV at 46 keV and ~2.2 keV at 1.33 MeV. The detector was calibrated with IAEA solid standards (RGU-1 and RGTh-1) for various geometries. The self-absorption corrections for the energy of interest were found to be negligible as evidenced by measurements of several standard reference materials and the close agreement between ^{226}Ra obtained using 352 keV (^{214}Pb) and 609 keV (^{214}Bi). This was verified by the measurements of ^{210}Po in an aliquot of

This is a preprint, the final version is subject to change, of the American Mineralogist (MSA)
Cite as Authors (Year) Title. American Mineralogist, in press.
(DOI will not work until issue is live.) DOI: http://dx.doi.org/10.2138/am-2017-6017

sample by dissolving and measuring by alpha spectrometry, under the assumption that ^{210}Po, ^{210}Pb, and ^{226}Ra are in secular equilibrium, as expected in any mineral older than 150 years. The total absorbed alpha dose (Δ, α-decays mg^{-1}) was calculated based on activities of each mineral sample using the following equation (Garver and Baskaran 2004):

$$\Delta = 8N_1\left[e^{\lambda_1 t} - 1\right] + 7N_2\left[e^{\lambda_2 t} - 1\right] + 6N_3\left[e^{\lambda_3 t} - 1\right] \quad (1)$$

where t is the geologic age of each mineral, N_1, N_2, and N_3 are the atoms mg^{-1} of ^{238}U, ^{235}U, and ^{232}Th, respectively, and λ_1, λ_2, and λ_3 are the decay constants (years^{-1}) for these respective isotopes. This calculation assumes 1) a closed system (no loss or gain of parent or daughter other than by radioactive decay) and 2) $N_2=N_1/137.88$ based on the natural abundances of ^{238}U and ^{235}U.

Radon emanation rate determination

Sample masses were aliquoted based on ^{238}U activities and ranged from 0.5-40 g. All samples were sealed off in a polyethylene vessel for three weeks in order to ensure steady state conditions between ^{226}Ra and ^{222}Rn (and its progeny) prior to measurement in the radon detector. The concentration of radon gas emission was measured using the RAD 7 Electronic Radon Detector (Durridge Company, Inc.) which has a calibration accuracy of ± 5% (Figure 1). The RAD 7 is a solid state alpha detector with a 0.7 liter internal sample cell volume. This instrument detects alpha particles released during radioactive decay and uses a semiconducting material to translate the energy into an electrical signal. The instrument records a spectrum of isotopic abundance based on each isotope's characteristic alpha decay energy (in MeV). The continuous monitoring feature provides statistically precise readings, and its ability to distinguish between "new radon" and "old radon" (via ^{218}Po versus ^{214}Po detection) prevents from any buildup

This is a preprint, the final version is subject to change, of the American Mineralogist (MSA)
Cite as Authors (Year) Title. American Mineralogist, in press.
(DOI will not work until issue is live.) DOI: http://dx.doi.org/10.2138/am-2017-6017

contaminating measurements in closed system setups. This setup consisted of a closed-loop system where the air pumped from the machine was passed through vinyl tubing to the sample vessel, followed by a series of filters and desiccators, and then back to the machine for counting (Figure 1). The relative humidity within the system, which is continually monitored by the RAD 7, was maintained below 10% at all times, and the continuous flow rate of air by the built-in air pump was 1 liter/minute. Cycle and recycle times varied between sets of mineral samples in order to account for large differences in ^{238}U activity. Cycles ranged from 30 to 60 minutes, and the total run time ranged from 24-72 hours. Once uploaded to RAD 7 data acquisition and analysis software (Capture, Durridge Company, Inc.), the default spill factors and sensitivities were replaced with specific values determined by each machine's calibration to increase the accuracy of the results. Background-subtracted radon measurements for each sample were used to calculate the REC value (%) based on the following equation:

$$REC = \frac{E}{N_{222}} * 100\% \quad (2)$$

where N_{222} is the number of ^{222}Rn atoms produced via ^{226}Ra and E is the ^{222}Rn emission rate (^{222}Rn atoms released per minute of RAD 7 run time), and is given by the following equation:

$$E = \frac{C}{\lambda_{222}} * \frac{v}{10^3} \quad (3)$$

where C is radon concentration per unit volume of air (Bq m^{-3}), v is flow rate (L min^{-1}), and λ_{222} is the decay constant for ^{222}Rn (s^{-1}) (Malczewski and Dziurowicz 2015).

This is a preprint, the final version is subject to change, of the American Mineralogist (MSA)
Cite as Authors (Year) Title. American Mineralogist, in press.
(DOI will not work until issue is live.) DOI: http://dx.doi.org/10.2138/am-2017-6017

RESULTS

Variations in ^{238}U, ^{232}Th activity, and total absorbed alpha dose

The measured ^{238}U and ^{232}Th activities are listed in Table 1. Uranium-238 activities range from 0.010 to 6487 Bq g^{-1} while ^{232}Th activities range from below detection limit (BDL) to 776 Bq g^{-1}. The activities of the zircon minerals ranged from 0.388 to 80.3 Bq g^{-1} of ^{238}U, which is within the wide range of activities reported for zircon minerals (~0.01 to >250 Bq g^{-1}) (Eakin et al. 2016). Thorium-232 activities for the zircons ranged from 0.235 to 39.6 Bq g^{-1}, which is slightly higher than previously reported values (~0.002 to ~20 Bq g^{-1}) (Eakin et al. 2016; Heaman and Parrish 1991). Thorite, euxenite, uraninite, and betafite had the highest activities (^{238}U range = 121 to 6487 Bq g^{-1}; ^{232}Th range = 53 to 776 Bq g^{-1}). The remaining seven minerals (hornblende, apatite, augite, microcline, albite, quartz, and olivine) had the lowest activities (^{238}U range = 0.010 to 1.52 Bq g^{-1}; ^{232}Th range: BDL to 1.08 Bq g^{-1}). Note that most common minerals (e.g. feldspar, quartz, and hornblende) have very low ^{238}U and ^{232}Th concentrations (Table 1, 2). No earlier published data was found on the uranium or thorium activities of euxenite, betafite, augite, microcline, albite, or olivine, and thus no comparison is possible. The calculated total absorbed alpha dose for the sample set ranged from 0.0036 to 2300 $x10^{15}$ decays mg^{-1} (Table 1). The corresponding values for silicates ranged from 0.0036 to 215 $x10^{15}$, oxides ranged from 217 to 2300 $x10^{15}$, and the phosphate was 0.480 $x10^{15}$ decays mg^{-1} (Table 1). Due to the overall similarity in geologic ages across the sample set, variations in alpha dose are primarily a result of variations in ^{238}U and ^{232}Th activities. The oxides have the three largest alpha dose values, and also have the three highest ^{238}U activities.

Radon Emanation Coefficients

The radon emanation coefficients for the analyzed mineral samples are given in Table 3. The REC values for different zircon grain-size fractions range from <0.01 to 0.77% (n=11, mean = 0.35%). Note that the lone REC value of 18.2% is an outlier, and is not included in the discussion. The REC values for <63, 63-125, 125-250, and 250-500 μm size fractions range from 0.27 to 0.77% (n=2, mean=0.53%), 0.21 to 0.72% (n=3, mean=0.44 %), 0.19 to 0.38 % (n=3, mean=0.31 %), and <0.01 to 0.35 % (n=3, mean=0.18 %), respectively. There is an inverse correlation between grain size and REC in all three zircon minerals. The REC values for the series of minerals heated from 200-800°C range from <0.01 to 0.58 % (n=35, mean = 0.16 %), and specific results are illustrated in Figure 2. The REC values resulting from heated mineral samples were generally highest upon heating to 300 or 400°C, and the lowest rates for all minerals (except euxenite) occurred upon heating to 600 or 800°C (Table 3, Figure 2). The Mud Tank zircon samples are excluded from this statement because all heated samples resulted in REC values of <0.01 %. 0.083 ± 0.03 at 25°C, 0.061 ± 0.003 % at 200°C,, 0.053 ± 0.003 % at 300°C,,0.062 ± 0.003 % at 400°C, 0.062 ± 0.003 % at 600°C,, and 0.109 ± 0.003 % at 800°C,

The REC range for a suite of 14 unheated mineral samples of <250μm grain sizes varied from 0.083 to 7.0% (mean=1.67%). This range is comparable to the previously reported range of <0.01 to 0.83% from a collection of 47 different studies comprising a total of 75 minerals (both bulk and pulverized); however, the present study includes a set of minerals that have never been measured before and that are expected to have very little radiative damage, which may be responsible for the higher REC values reported (Sakoda et al. 2011). The REC for unheated silicates of <125-250 μm ranged from 0.19 to 7.0% (n=9, mean=1.89%). For oxides, the REC ranged from 0.083 to 0.177% (n=3, mean=0.14%), and the REC value of the phosphate mineral

This is a preprint, the final version is subject to change, of the American Mineralogist (MSA)
Cite as Authors (Year) Title. American Mineralogist, in press.
(DOI will not work until issue is live.) DOI: http://dx.doi.org/10.2138/am-2017-6017

was found to be 5.4 ± 0.1%. The silicate group produced a wide range of REC values as well as the highest REC values. The oxide group showed a narrow range of low REC values and is composed of minerals with higher ^{238}U and ^{232}Th activities. Zircon had the lowest REC among all the minerals listed in Table 1, similar to what has been reported elsewhere (Sakoda et al. 2011; Garver and Baskaran, 2004; Eakin et al., 2016). Commonly-occurring minerals such as hornblende and quartz with very low ^{238}U and ^{232}Th activities have mean REC values of 2.2% and 4.3%, respectively, which are higher than the values reported for uraninite and zircon (Table 2, 3). The REC value for quartz (3.8 ± 0.5%) is similar to the value reported by Sakoda et al. (2010) of 4.6 ± 0.5%; the measured value for hornblende is lower (0.90 ± 0.03%) compared to the published value of 3.42 ± 0.38% (Krishnaswami and Seidemann, 1988); and the value for apatite reported in this study is much higher (5.4 ± 0.11%) compared to 0.5 and 0.8% from a study by Rama (1990a)) (Table 2). Some of the minerals included in this experiment are known to commonly occur as accessory minerals (euxenite, zircon, and thorite), which exhibit heterogeneous ^{226}Ra distribution, leading to variable REC values. However, many of these samples were single crystals and were pulverized and thus, this should not be a factor (unless crushing resulted in breaking along cleavage plane and the heterogeneity is preserved in the crushed grains). The range of reported REC of zircon (both in air and solution) vary over six orders of magnitude, while that of uraninite and thorite vary over five and three orders of magnitude, respectively (Table 2).

This is a preprint, the final version is subject to change, of the American Mineralogist (MSA)
Cite as Authors (Year) Title. American Mineralogist, in press.
(DOI will not work until issue is live.) DOI: http://dx.doi.org/10.2138/am-2017-6017

DISCUSSION

A number of factors affect radon emanation rates, including particle size and shape, internal porosity, the extent of radiation damage within the crystalline structure, the type of distribution of impurities and imperfections in the crystal lattice, and the concentration and distribution of ^{226}Ra (Tanner, 1980; Strong and Levins, 1982; Rama and Moore, 1984; Krishnaswami and Seidemann, 1988; Rama and Moore, 1990a; Garver and Baskaran, 2004; Lawrence et al., 2009; Eakin et al., 2016). For example, in the case of zircon, the effects of alpha-decay damage on zircon were reported to include decrease in density (17%), decrease in hardness, decrease in thermal conductivity, increase in adsorbed water, increase in chemical diffusion, and increased susceptibility (Murakami et al., 1991; Weber et al., 1994). Furthermore, release rates of radon outside of a mineral grain also depend on the surrounding medium (air or water; Tanner, 1964). There are heterogeneities in the distribution of uranium isotopes in U-bearing minerals, where the isotopes are commonly concentrated in certain localized regions of the mineral depending on its mode of formation and whether or not recrystallization occurred (e.g., Sakoda et al., 2010). Furthermore, the progeny of ^{238}U are likely to lie in the recoil tracks along which the mineral is chemically and structurally ruptured (note that ^{238}U reside in crystalline material while the progeny (up to ^{206}Pb) will not be). Rama and Moore (1990a) observed large radon emanation coefficients from crystals of apatite, uraninite and monazite and argued that these results provide evidence for existence of micro-crystallinity and associated network of internal gaps (or pores) that are extremely narrow (nm wide) due to extremely low porosity in these minerals and are connected to the surface. From a diffusion study of ^{220}Rn across nanometer wide holes in common rock minerals, Rama and Moore (1990b) reported that the zones of porosity are circuitous and thus, the effective diffusion length of ^{220}Rn and ^{222}Rn are

This is a preprint, the final version is subject to change, of the American Mineralogist (MSA)
Cite as Authors (Year) Title. American Mineralogist, in press.
(DOI will not work until issue is live.) DOI: http://dx.doi.org/10.2138/am-2017-6017

~ 3mm and 30 cm, respectively in granite, compared to the corresponding values in air of 3 cm and 3 m, respectively. Different factors that affect radon emanation rates of minerals are discussed below.

REC variations in water and air

The release rates of radon outside of a mineral grain depend on the surrounding medium (air or water; Tanner, 1964). Radon emanation coefficients obtained in air can be compared to the REC values for the same set of mineral aliquots obtained in water (Eakin et al. 2016) (Table 2). The REC values in water are distinctively higher than that in air (Table 2). Higher values of REC in water are likely due to the presence of water in pore spaces (note that the size of a water molecule is 0.29 nm), which increases the probability that radon atoms will terminate their recoil paths in those spaces due to a shorter stopping distance in water than in air, thus augmenting the direct-recoil fraction. This indicates that radon atoms emanating in air are much more likely to be embedded into adjacent grains.

While minerals such uraninite containing very high ^{238}U concentrations can become amorphous (metamict) due to self-irradiation by decaying actinides, minerals such as zircon (and monazite with high ^{232}Th concentrations) have remarkable stability, although residual atomic displacement damage produced by alpha recoil atoms could accelerate the actinide dissolution affecting the distribution of ^{226}Ra and thereby the release rates of radon. Radon emanation coefficients as high as 12.1% and 23% for the much shorter-lived ^{220}Rn (Barretto, 1973) have been reported, although, in general, the radon emanation coefficients for zircon are much lower (e.g., Eakin et al., 2016). Due to this high REC value, we speculate that the effect of radiation

This is a preprint, the final version is subject to change, of the American Mineralogist (MSA)
Cite as Authors (Year) Title. American Mineralogist, in press.
(DOI will not work until issue is live.) DOI: http://dx.doi.org/10.2138/am-2017-6017

damage is to form a mosaic of channels in which water may be introduced to increase the direct-recoil fraction, or along which the mineral may be altered resulting in potential increase in the indirect-recoil and diffusion fractions. It is also documented that recoil tracks are responsible for a portion of the preferential removal of ^{234}U by water entering through these recoil tracks and healing of such tracks by heating could diminish the release of nuclides such as ^{234}U and ^{226}Ra (e.g. Fleischer 1982) which also result in the increase in radon release rates.

REC values as a function of grain size

When the grain size is smaller than radon recoil distance, almost all of the radon released from recoil will escape the grain. The contribution of radon escape from solid state diffusion (assuming that there is preferential diffusion through nanopores or recoil/alpha nuclear tracks or radiation damage inside a grain) is expected to be small due to diffusion length ($= \sqrt{(D\tau)}$ where D_s is diffusion coefficient of ^{222}Rn in solids, $10^{-25} – 10^{-27}$ m^2 s^{-1}, summarized in Baskaran, 2016) and τ is mean-life of ^{222}Rn (5.51 d)) is ~ 0.02-0.2 nm. The recoil length of radon atoms is 30-50nm and hence radon emanation by recoil is in effect a surface phenomenon (upper 50 nm) (Semkow 1991; Malczewski and Dziurowicz 2015). If the volume of the surface layer of a mineral grain is ~0.01% of the total volume, the mean grain size for each fraction tested in this study would result in ^{222}Rn escape by recoil to be less than ~0.0001%. However, a consistent inverse relationship was observed between REC and grain size, where REC values increase with decreasing grain size and thus larger surface area per volume (Table 3). This implies that recoil rather than diffusion is responsible for the majority of radon escape from the samples. The

This is a preprint, the final version is subject to change, of the American Mineralogist (MSA)
Cite as Authors (Year) Title. American Mineralogist, in press.
(DOI will not work until issue is live.) DOI: http://dx.doi.org/10.2138/am-2017-6017

fraction of radon emitted as a result of recoil can be related to the grain size of homogeneous, spherical, defect-free grains is given by (Giletti and Kulp 1954):

$$F_r = \frac{3}{4}\frac{R}{r_o} - \frac{1}{16}\left(\frac{R}{r_o}\right)^3 for\ 2r_o \geq R \quad (4)$$

where F_r is the fraction of radon atoms emitted due to recoil, R is recoil range, and r_o is the radius of the grain. From equation (4), the fraction of radon atoms emitted as a function of grain size for a recoil range of 50 nm yields an inverse relationship between surface area and the radon emanation rate. However, such a relationship is not commonly reported, primarily because no study has been conducted with grain sizes in the range of 0.05 – 1 μm. For example, REC from a 30 cm x 30 cm x 30 cm cube of granite was reported to be the same as that for a 1-2 mm granite sample (Amin and Rama 1986). Two hypotheses have been proposed to account for the discrepancy between expected and measured radon emanation rates: 1) heterogeneous ^{226}Ra distribution, or 2) a network of nanopores aiding in gas transport within the mineral (Rama and Moore 1984). These nanopores would increase the internal surface area of the mineral, allowing for a higher amount of radon diffusion, resulting in greater emanation in smaller grains due to higher surface area to volume ratios. Furthermore, the zones of nano-porosity have been suggested to form a network that connects to the grain boundary (Rama and Moore 1990). In low-temperature-formation minerals such as quartz and feldspars, the submicronic porosity is reported to be 10-20% while in amphiboles, the entire inner area is leaky and hence radon escape is expected to be higher (Rama and Moore, 1990b). Thus, the radon emanation could depend on the fraction of submicronic porosity (fractional volume of mineral exhibiting submicronic porosity) since the zones of submicron porosity are reported to run both along grain boundaries and across the grains (Rama and Moore 1990b). In order to account for the concentration of

This is a preprint, the final version is subject to change, of the American Mineralogist (MSA)
Cite as Authors (Year) Title. American Mineralogist, in press.
(DOI will not work until issue is live.) DOI: http://dx.doi.org/10.2138/am-2017-6017

330 ^{226}Ra at grain boundaries, the fraction of radon atoms emitted by recoil ($F_{uniform}$) is given by
331 (Morawska and Phillips 1993):

332 $$F_{uniform} = 0.5 * (1 + \frac{R}{d}) \quad (5)$$

333 where d is the diameter of the mineral grain. The range of grain diameters used in this study
334 produced an F value approximating 0.5 for each size fraction (note that the variations in
335 calculated REC values remain more or else constant for grain sizes of 63 and 500 μm), which
336 would produce a constant REC value for the samples tested. Therefore, another mechanism such
337 as nanopores or radiation damage which could increase the surface area to volume ratio with
338 decreasing grain size compared to a defect-free grain must be responsible for the REC values
339 reported in this study

340

341 **REC values as a function of temperature**

342 It is known that alpha recoil tracks anneal much more readily than fission tracks when a
343 mineral is subjected to elevated temperatures. Hasheminezhad and Durrani (1983) determined
344 that 100% annealing of alpha tracks in biotite occurred at a finite temperature, with activation
345 energy of 1.4 eV. The corresponding activation energy for fission tracks is much higher, and
346 thus, a much higher temperature is required for complete annealing (Hasheminezhad and Durrani
347 1983). In our study, in five of the seven heated minerals, an increase in REC between 300 and
348 400°C is observed which may correspond to complete annealing of α-recoil tracks. It was
349 demonstrated that the heating of zircon minerals over an extended period of time (>24 h) can
350 change the crystal structure through annealing of α-recoil and fission tracks (Yamada et al.

This is a preprint, the final version is subject to change, of the American Mineralogist (MSA)
Cite as Authors (Year) Title. American Mineralogist, in press.
(DOI will not work until issue is live.) DOI: http://dx.doi.org/10.2138/am-2017-6017

1995). The network of interconnected fission and α-recoil tracks in uranium and thorium-bearing minerals is proposed to result in the formation of channels serving as conduits for ^{222}Rn gas escape. Partial annealing of all the tracks (at low temperatures, mostly α-recoil tracks) may temporarily relieve "congestion" (analogous to a traffic jam) which could lead to higher REC values prior to full fission track annealing. However, Eakin et al. (2016) also reported decrease in REC with partial annealing in one of the three zircon samples studied. Garver and Baskaran (2004) showed that for monazite, zircon, and uraninite, the REC values followed the trend: 200°C > 100°C > 600°C. In the case of zircon, the least amount of variation in the REC value was reported at different degrees of heating (Garver and Baskaran 2004, Eakin et al. 2016). From the differences in the amount of radon released from a zircon sample heated twice (with a time gap of about a month) at 975°C for 48 hours, Eakin et al. (2016) suggested that diffusion parameters are changed due to annealing of radiation damage. When the heating temperature approaches the total annealing temperature, the nuclear track-induced channels are likely removed, resulting in lower REC values. The REC value of Mud Tank zircon, upon any degree of heating, was <0.01%, perhaps due to the low activity of the mineral and lack of significantly interconnected fission tracks. The euxenite sample lacked any trend in REC values with an increase in temperature. Euxenite, a complex uranium yttrium oxide with many substitution sites within its chemical formula (termed the "trash can mineral") is likely influenced by other chemical or physical properties from the higher concentrations of other elements present which are affecting the radon emanation rates. Furthermore, complete recrystallization of euxenite could occur at much greater than 1000°C at laboratory conditions and timescales and therefore the degree of annealing for each sample likely varied, especially if any minerals experienced

This is a preprint, the final version is subject to change, of the American Mineralogist (MSA)
Cite as Authors (Year) Title. American Mineralogist, in press.
(DOI will not work until issue is live.) DOI: http://dx.doi.org/10.2138/am-2017-6017

long term annealing by geothermal events in the natural environment, independent of laboratory annealing (Murakami et al. 1991).

REC values as a function of U-Th concentration and alpha dose

The minerals in this study show an R^2 value of 0.53 (polynomial fit) for REC versus activity concentrations of ^{238}U and 0.49 for REC versus alpha dose, indicating a weak linear relationship between REC and both parameters (Figure 3, Figure 4). There is no relationship between REC and the activity of ^{238}U, ^{232}Th, or alpha dose in a recent study by Eakin et al. (2016) on zircons; however, an inverse relationship was observed between REC and radiation dose by Malczewski and Dziurowicz (2015). Variations in mineral composition and lattice structure will likely affect radon emanation along with radiation dose. For example, the uraninite sample in the Malczewski and Dziurowicz study (2015) had the highest ^{238}U activity and radiation dose but the lowest REC value, similar to this study. The authors proposed that due to uraninite's simple and compact oxide structure, this mineral is essentially dose-independent. All of the oxides in this study produced low REC values despite their high ^{238}U concentrations. Silicates have more complex crystal lattice structures, and also exhibited a higher variability of REC despite lower activity, further suggesting the influence of mineral structure and composition on radon emanation rates (Figures 3, 4).

REC dependence on melting point and density

This is a preprint, the final version is subject to change, of the American Mineralogist (MSA)
Cite as Authors (Year) Title. American Mineralogist, in press.
(DOI will not work until issue is live.) DOI: http://dx.doi.org/10.2138/am-2017-6017

393 The melting point and density of a mineral depends on the covalent bonding energy and
394 the lattice arrangement of atoms within that mineral. It is anticipated that those minerals with
395 high melting point and density will likely have lower radon emanation coefficients. Based on the
396 variability of REC with activity, alpha dose, and nuclear track annealment, it is likely that the
397 physical structure of a mineral is influential in the degree of radon emanation. A mineral's
398 density and melting point are directly related, as both parameters are based on how tightly-
399 packed the atoms of the mineral are. A more compact internal mineral structure should inhibit
400 the mobility of radon atoms and thus lower emanation rates. Figure 5 and Figure 6 show the REC
401 versus density and melting point for the minerals in this study. Neither parameter correlates
402 significantly with REC (R^2=0.17 for REC versus density; R^2=0.044). Minerals with similar
403 densities but a wide range of activity concentrations show a correspondingly wide range of REC
404 values, which span over three orders of magnitude (Table 1, 3; Figure 5). This variability is
405 reduced at the lowest and highest extents of density (the uraninite sample has the highest density
406 and lowest REC value, and the mineral samples with densities of <2 showed relatively high REC
407 values). When REC is compared to minerals with melting points of 1400°C and higher, the R^2
408 value increases to 0.52 (with the exclusion of betafite, R^2=0.77), indicating a much stronger
409 correlation (Figure 6). It is thus proposed that minerals with lower melting points (and densities)
410 are prone to more variable lattice structures by radiative damage or other physical defects,
411 resulting in a wider range of REC values, whereas higher density minerals such as uraninite
412 exhibit REC values that are more strongly controlled and limited by their physical structure.

413

414

This is a preprint, the final version is subject to change, of the American Mineralogist (MSA)
Cite as Authors (Year) Title. American Mineralogist, in press.
(DOI will not work until issue is live.) DOI: http://dx.doi.org/10.2138/am-2017-6017

IMPLICATIONS

Understanding the physical and mineralogical processes which control radon emanation from minerals is essential to obtain reliable ^{238}U-^{206}Pb and U-He ages on individual minerals. Furthermore, the results presented in this article are important and relevant for understanding the mechanism of ^{222}Rn loss from different minerals and have potential implications for the discordant ages obtained from ^{206}Pb/^{228}U-^{207}Pb/^{235}U-^{208}Pb/^{232}Th pairs. Furthermore, the radon release rate from continents/ocean surface has direct bearing on the production of rates of ^{210}Pb from the decay of ^{210}Pb and hence applications of ^{210}Pb and ^{222}Rn as atmospheric circulation tracers require a thorough understanding of the factors that control the release rates of ^{222}Rn from soils and minerals.

The presented results indicate that specific factors such as grain size, heating, and melting point can have a direct bearing on the amount of radon released. In addition, nanopores or radiative damage in minerals can amplify the relationship between REC emanation and grain size. Radiation damage promotes the release of radon due to an increased internal surface area of minerals. Here we propose that partial annealing of fission tracks can increase radon emanation rates by relieving congestion within crystal lattices, while full annealing decreases emanation rates by eliminating pathways for radon release. The results of this study indicate that high density minerals produce the lowest REC values and low density minerals produce higher REC values; however, the trend is not consistently observed and thus other chemical and physical properties complicate this relationship. Minerals with higher melting points (≥1400°C) are inversely related to REC values, as expected based on mineral density. Minerals with a lower melting point and density are prone to greater chemical and physical variability, and for these reasons, REC values are also subject to a greater degree of variability.

This is a preprint, the final version is subject to change, of the American Mineralogist (MSA)
Cite as Authors (Year) Title. American Mineralogist, in press.
(DOI will not work until issue is live.) DOI: http://dx.doi.org/10.2138/am-2017-6017

Radon isotopes that have longer half-lives have a higher probability of being lost before decaying to their progeny, so we expect longer half-lives to equate to higher REC values, and following from linear diffusion theory, it is anticipated that the REC for ^{219}Rn, ^{220}Rn and ^{222}Rn will be in rough proportion to the square root of their half-lives (i.e., 1.0:3.7:290). Significant deviations from these expected values could aid in probing the heterogeneity in the distribution of their precursors (^{223}Ra, ^{224}Ra and ^{226}Ra, respectively). Therefore, our future studies are focused in understanding the factors and processes that cause variations in the RECs values for ^{219}Rn and ^{220}Rn.

Acknowledgements: This work was performed as an undergraduate research project supported by an REU in NSF grant (OCE-1237059, PI: MB). We thank the two anonymous reviewers for their insightful reviews.

References

Amin, B.S., and Rama (1986) Using radon as probe for investigating characteristics of fractures in crystalline minerals. Nuclear Instruments and Methods in Physics Research, B17, 527-529.

Broecker, W.S., Li, Y.H., and Cromwell, J. (1967) Radium-226 and radon-222 – concentration in Atlantic and Pacific oceans. Science, 158, 1307-1310.

Baskaran, M. (2016) Mechanisms of radon emanation and long-term radon flux studies. In: *Radon: A Tracer for Geological, Geophysical and Geochemical Studies* -Baskaran – August 2016 (Book DOI: 10.1007/978-3-319-21329-3; ISBN: 978-3-319-21328-6; Springer, Switzerland.

Corfu, F. (2012) A century of U-Pb geochronology: the long quest towards concordance. Geological Society of America Bulletin, 125, 33-47.

Eakin, M., Brownlee, S.J., Baskaran, M., and Barbero, L. (2016) Mechanisms of radon loss from zircon: microstructural controls on emanation and diffusion. Geochemica et Cosmochimica Acta, 184, 212-226.

Fleischer, R. L. (1982) Nature of alpha-recoil damage – evidence from preferential solution effects. Nuclear Tracks and Radiation Measurements, 6, 35-42.

Fleischer, R.L., and Turner, L.G. (1984) Correlations of radon and carbon isotopic measurements with petroleum and natural-gas at cement, Oklahoma. Geophysics, 49, 810-817.

Fleischer, R.L., and Mogrocampero, A. (1985) Association of subsurface radon changes in Alaska and the northeastern United States with earthquakes. Geochemica et Cosmochimica Acta, 49, 1061-1071.

Garver, E., and Baskaran, M. (2004) Effects of heating on the emanation rates of radon-222 from a suite of natural minerals. Applied Radiation and Isotopes, 61, 1477-1485.

Giletti, B.J., and Kulp, J.L. (1954) Radon leakage from radioactive minerals. Lamont Geological Observatory Contribution No. 162.

Goa, Y., Li, X., Griffin, W.L., O'Reilly, S.Y., and Wang, Y. (2014) Screening criteria for reliable U-Pb geochronology and oxygen isotope analysis in uranium-rich zircons: A case study from the Suzhou A-type granites, SE China. Lithos, 192-195, 180-191.

Hasheminezhad, S.R. and Durrani, S.A. (1983) Annealing behavior of alpha-recoil tracks in biotite mica – implications for alpha-recoil dating method. Nuclear Tracks and Radiation Measurements, 7, 141-146.

Heaman, L., and Parrish, R. (1991) U-Pb geochronology of accessory minerals. In: Heaman, L., Ludden, J.N. (eds) Applications of Radiogenic Isotope Systems to Problems in Geology, pp 59-102. Mineralogical Association of Canada, Nepean.

Heaman , L.M., and LeCheminant, A.N. (2000) Anomalous U-Pb systematics in mantle-derived baddeleyite xenocrysts from He Bizard: evidence for high temperature radon diffusion? Chemical Geology, 172, 77-93.

Krishnaswami, S., and Seidemann, D.E. (1988) Comparative study of ^{222}Rn, ^{40}Ar, ^{39}Ar and ^{37}Ar leakage from rocks and minerals: implications for the role of nanopores in gas transport through natural silicates. Geochemica et Cosmochimica Acta, 52, 655-658.

Kritz, M.A., Rosner, S.W., Kelly, K.K., Loewenstein, M., and Chan, K.R. (1993) Radon measurements in the lower tropical stratosphere: evidence for rapid vertical transport and dehydration of tropospheric air. Journal of Geophysical Research, 98, 8735-8736.

Lawrence, C.E., Akber, R.A., Bollhofer, A., and Martin, P. (2009) Radon-222 exhalation from open ground on and around a uranium mine in the wet-dry tropics. Journal of Environmental Radioactivity, 100, 1-8.

Levinson, A.A., Bland, C.J., and Lively, R.S. (1982) Exploration for U Ore Deposits, In: Ivanovich, M., Harmon, R.S. (eds) Uranium Series Disequilibrium, pp 351-383. Clarendon Press, Oxford.

Lide, D.R., Ed. (1998) CRC Handbook of Chemistry and Physics, 79th ed, CRC Press, Boca Raton, Florida.

Lipin, B.R. (1984) Chromite from the Blue Ridge Province of North Carolina. American Journal of Science, 284, 507-529.

Liu, S.C., McAffee, J.R., and Cicerone, R.J. (1984) Radon-222 and tropospheric vertical transport. Journal of Geophysical Research, 89, 7291-7297.

Malczewski, D., and Dziurowicz, M. (2015) ^{222}Rn and ^{220}Rn emanations as a function of the absorbed alpha-doses from select metamict minerals. American Mineralogist, 100, 1378-1385.

512 Mazeina, L., Ushakov, S.V., Navrotsky, A., and Boatner, L.A. (2005) Formation enthalpy of
513 $ThSiO_4$ and enthalpy of the thorite → huttonite phase transition. Geochimica et
514 Cosmochimica Acta, 69, 4675-4683.

515 Médard, E., Schmidt, M.W., Schiano, P., and Ottolini, L. (2005) Melting of amphibole-bearing
516 wehrlites: an experimental study on the origin of ultra-calcic nepheline-normative melts.
517 Journal of Petrology, 47, 481-504.

518 Mezger, K., Essene, E.J., van der Pluijm, B.A., and Halliday, A.N. (1992) U-Pb geochronology
519 of the Grenville Orogen of Ontario and New York: constraints on ancient crustal
520 tectonics. Contributions to Mineralogy and Petrology, 114, 13-26.

521 Morawska, L, and Phillips, C.R. (1993) Dependence of the radon emanation coefficient on
522 radium distribution and internal structure of the material. Geochimica et Cosmochimica
523 Acta, 57, 1783-1797.

524 Murakami, T., Chakoumakos, B.C., Ewing, R.C., Lumpkin G.R., and Weber, W.J. (1991) Alpha-
525 decay event damage in zircon. American Mineralogist, 76, 1510-1532.

526 Nazaroff, W.W. (1992) Radon transport from soil to air. Reviews of Geophysics, 30, 137.

527 Nyman, M.W., Karlstrom, K.E., Kirby, E., and Graubard, C.M. (1994) Mesoproterozoic
528 contractional orogeny in western North America: Evidence from ca. 1.4 Ga Plutons.
529 Geology, 22, 901-904.

530 Opta Minerals Inc. (2015) Zircon Sands: Characteristics. Retrieved from:
531 www.optaminerals.com/Foundry/Zircon-Sand.html.

Powell, W.G. (n.d.) Minerals and their physical properties: Igneous rocks and properties [7040 lecture 6]. Department of Earth and Environmental Sciences, Brooklyn College, Brooklyn, New York.

Rama, and Moore, W.S. (1984) Mechanism of transport of U-Th series radioisotopes from solids into ground water. Geochimica et Cosmochimica Acta, 48, 395-399.

Rama and Moore, W.S. (1990a) Micro-cystallinity in radioactive minerals. Nuclear Geophysics, 4, 475-478.

Rama and Moore, W.S. (1990b) Submicronic porosity in common minerals and emanation of radon. Nuclear Geophysics, 4, 467-473.

Sakoda, A., Ishimori, Y., Hanamoto, K., Kataoka, T., Kawabe, A., and Yamaoka, K. (2010) Experimental and modeling studies of grain size and moisture content effects on radon emanation. Radiation Measurements, 45, 204-210.

Sakoda, A., Ishimori, Y. and Yamaoka, K. (2011) A comprehensive review of radon emanation measurements for mineral, rock, soil, mill tailing, and fly ash. Applied Radiation and Isotopes, 69, 1422-1435.

Semkow, T.M. (1990) Recoil-emanation theory applied to radon release from mineral grains. Geochimica et Cosmochimica Acta, 54, 425-440.

Semkow, T.M. (1991) Fractal model of radon emanation from solids. Physical Review Letters, 66, 3012-3015.

Strong, K.P. and Levins, D.M. (1982) Effect of moisture content on radon emanation from uranium ore and tailings. Health Physics, 42, 27-32.

Tanner, A.B. (1964) Radon migration in the ground: a review. In: Adams, J.A.S., and Lowder, W.M. (eds.) The Natural Radiation Environment, pp161-190. The University of Chicago Press, Illinois.

Tanner, A.B. (1980) Radon migration in the ground: a supplementary review. In: Gessel, T.F., and Lowder, W.M. (Eds.) Natural Radiation Environment III, Symposium Proceedings, pp. 5-56. CONF-780422, Springfield, Virginia.

Thomas Jefferson National Accelerator Facility – Office of Science Education. (n.d.) The element Terbium. Retrieved from: education.jlab.org/itselemental/ele065.html

Turekian, K.K., Nozaki, Y., and Benninger, L.K. (1977) Geochemistry of atmospheric radon and radon products. Annual Review of Earth and Planetary Sciences, 5, 227-255.

Wakita, H., Igarisha, G., and Notsu, K. (1991) An anomalous radon decrease in groundwater prior to an M6.0 earthquake – a possible precursor. Geophysical Research Letters, 18, 629-632.

Weast, R.C., Ed. (1981) CRC Handbook of Chemistry and Physics, 62nd Edition, CRC Press, Boca Raton, Florida.

WHO (World Health Organization) (2009) WHO handbook on indoor radon – a public health perspective. In: Hajo Z, Ferid S (eds).

Weber, W.J., Ewing, R.C., and Wang, L.M. (1994) The radiation-induced crystalline-to-amorphous transition in zircon. Journal of Materials Research, 9, 688-698.

573 Xiao, H.Y., Weber, W.J., Zhang, Y., Zu, X.T., and Li, S. (2015) Electronic excitation induced
574 amorphization in titanate pyrochlores: an *ab initio* molecular dynamics study. Scientific
575 Reports, 5, 1-8.

576 Yamada, R., Tagami, T., Nishimura, S., and Ito, H. (1995) Annealing kinetics of fission tracks in
577 zircon – an experimental study. Chemical Geology, 122, 249-258.

578

This is a preprint, the final version is subject to change, of the American Mineralogist (MSA)
Cite as Authors (Year) Title. American Mineralogist, in press.
(DOI will not work until issue is live.) DOI: http://dx.doi.org/10.2138/am-2017-6017

List of Figure Captions

Figure 1. RAD 7 experimental set-up. Air is pumped from RAD-7 into the sample vessel in a closed-loop by vinyl tubing, followed by an air filter to prevent mineral grains from migrating through the system, and a desiccator. Air is then returned into RAD-7 for counting.

Figure 2: Radon emanation coefficient (%, average value used for plots) as a function of temperature. The linear fit is given for the full dataset as well as a partial dataset (which excludes REC values at 200° and 300°C). Error bars are included for all data points (not visible in cases when errors are smaller than the symbol size). Mud Tank zircon dataset is not included due to below detection level of radon emanation upon heating.

Figure 3: A plot of radon emanation coefficient as a function of ^{238}U activity for all unheated minerals. Error bars are included for all data points (not visible in cases when errors are smaller than the symbol size).

Figure 4: A plot of radon emanation coefficient versus total absorbed alpha dose for all unheated mineral samples. Error bars are included for all data points (not visible in cases when errors are smaller than the symbol size).

Figure 5. The radon emanation rate as a function of density for all unheated minerals of <250 μm. Error bars are included for all data points (not visible in cases when errors are smaller than the symbol size).

Figure 6: The radon emanation coefficient as a function of melting point (data in Table 3) for 1) all unheated minerals (red), 2) mineral samples with melting points ≥ 1400°C (blue), and 3) for minerals with melting points ≥1400°C, excluding betafite (green). There is no significant correlation for the whole sample set, but for minerals with ≥ 1400°C melting temperature, there is a significant correlation.

This is a preprint, the final version is subject to change, of the American Mineralogist (MSA)
Cite as Authors (Year) Title. American Mineralogist, in press.
(DOI will not work until issue is live.) DOI: http://dx.doi.org/10.2138/am-2017-6017

Table 1. Location, specific gravity, melting point, activities of measured ^{238}U and ^{232}Th, and calculated total absorbed alpha dose on a suite of minerals. Uncertainties are propagated from counting statistics.

Mineral	Locality	Chemical Formula	Specific Gravity (Melting Point, °C)	Estimated Age (Ma)	^{238}U Activity (Bq g^{-1})	^{232}Th Activity (Bq g^{-1})	Total Alpha Dose ($x10^{15}$) (decays mg^{-1})
Euxenite	Chaffee County, Colorado	$(Y,Ca,Ce,U,Th)(Nb,Ti,Ta)_2O_6$	4.85(1356[5])	ca.1400[10]	395 ± 2	180 ± 1	217 ± 2
Uraninite	Bancroft, Ontario, Canada	UO_2	11(2827[4])	ca. 1150[8]	6487 ± 49	446 ± 3	2300 ± 29
Betafite	Bancroft, Ontario, Canada	$(Ca,U)_2(Ti,Nb,Ta)_2O_6(OH)$	4.3(1602[3])	ca.1150[8]	2283 ± 17	53 ± 1	786 ± 17
Thorite	Bancroft, Ontario, Canada	$(Th,U)SiO_4$	5.3(1200[6])	ca.1150[8]	121 ± 1	776 ± 5	215 ± 3
Zircon	Malawi, Africa	$ZrSiO_4$	4.67(2200[7])	730 ± 20[9]	8.87 ±0.07	4.13 ± 0.10	2.4 ± 0.1
	Bancroft, Ontario, Canada			1050 ± 12	80.3 ± 0.6	39.6 ± 0.9	33 ± 1
	Mud Tank, Australia			732 ± 5	0.388 ±0.008	0.235 ± 0.027	0.113 ± 0.013
Hornblende	Bancroft, Ontario, Canada	$(Ca,Na)_{2-3}(Mg,Fe,Al)_5(Si,Al)_8O_{22}(OH,F)_2$	2.9-3.5(1100[2])	ca. 1200[8]	1.52 ±0.01	0.308 ± 0.006	0.61 ± 0.01
Augite	Bancroft, Ontario, Canada	$(Ca,Na)(Mg,Fe^{2+},Al,Fe^{3+},Ti)[(Si,Al)_2O_6]$	3.19-3.56(1400[1])	ca. 1200[8]	0.069 ± 0.001	0.021 ± 0.001	0.035 ± 0.002
Microcline	Bancroft, Ontario, Canada	$KAlSi_3O_8$	2.54-2.63(1250[1])	ca. 1200[8]	0.465 ± 0.004	0.021 ± 0.002	0.17 ± 0.02
Albite	Madawaska, Ontario, Canada	$NaAlSi_3O_8$	2.76(1100[1])	ca. 1200[8]	0.0103 ± 0.0003	0.0010 ± 0.0004	0.0039 ± 0.0016
Quartz	Bancroft, Ontario, Canada	SiO_2	2.65(1600[1])	ca. 1200[8]	0.0177 ± 0.0005	BDL*	0.00629 ± 0.00025
Olivine (via Dunite)	Jackson county, North Carolina	$(Fe,Mg)_2SiO_4$	3.22-4.39(1800[1])	1100-1300[11]	0.010 ± 0.001	BDL	0.00356 ± 0.00050
Apatite	Bancroft, Ontario, Canada	$Ca_5(PO_4)_3(F,OH,Cl)$	2.9-3.5(1600[1])	ca. 1200[8]	0.64 ± 0.01	1.08 ± 0.01	0.480 ± 0.012

*Below detection limit.

[1]Powell, n.d. [2]Médard et al., 2005 [3]Xiao, 2015 [4]Lide, 1998; Weast, 1981 [5]Thomas Jefferson National Accelerator Facility, n.d. [6]Mazeina et al. 2005 [7]Opta Minerals Inc. 2015.
[8]Mezger et al., 1992 [9]Eakin et al., 2016 [10]Nyman et al., 1994 [11]Lipin, 1984.

This is a preprint, the final version is subject to change, of the American Mineralogist (MSA)
Cite as Authors (Year) Title. American Mineralogist, in press.
(DOI will not work until issue is live.) DOI: http://dx.doi.org/10.2138/am-2017-6017

609 Table 2. Comparison of the activities of ^{238}U, ^{232}Th, and radon emanation coefficients in different size fractions determined in this study with the values reported in literature.*

Mineral	Locality	Estimated Age (MA)	Size Fraction (μm)	U-238 (Bq/g)	Th-232 (Bq/g)	Radon Emanation Coefficient (%)	Reference
Uraninite	Wilberforce, Ontario	1000 ± 200	<63	5829 ± 69	376.73 ± 7.32	0.53 ± 0.01	Garver et al. 2004
			1000-2000			0.53 ± 0.01	
	Oklo, Gabon	1968 ± 50	bulk	9465 ± 216	5.1 ± 2	0.000049	Malczewski et al. 2015
	NA	NA	NA	6550	NA	1.9	Rama 1990a
	Bancroft, Ontario	ca. 1150	125-250	6487 ± 49	446 ± 3	0.18 ± 0.001	This study
Zircon	Malawi, Africa	730 ± 20	125-250	8.87 ± 0.07	4.13 ± 0.1	2.21 ± 0.23	Eakin et al. 2016
			125-250			0.37 ± 0.02	This study
	Bancroft, Ontario	1050 ± 12	125-250	80.27 ± 0.58	39.58 ± 0.87	2.11 ± 0.35	Eakin et al. 2016
			125-250			0.19 ± 0.01	This study
	Mud Tank, Australia	732 ± 5	125-250	0.388 ± 0.008	0.235 ± 0.027	1.76 ± 0.64	Eakin et al. 2016
			125-250			0.38 ± 0.2	This study
	Goias, Brazil	2900 ± 200	<63	50.1 ± 0.5	4.6 ± 0.1	1.04 ± 0.01	Garver et al. 2004
			1000-2000			0.47 ± 0.01	
	NA	NA	NA	3.831 ± 2.986	NA	0.01 ± 0.00	Rama 1990a
	NA	NA	NA	NA	NA	0.2 – 4.8	Barretto 1973
	NA	NA	NA	NA	NA	12.1	
Thorite	Tory Hill, Ontario	1000 ± 200	<63	104 ± 2	869 ± 9	5.38 ± 0.08	Garver et al. 2004
	Cardiff Twp, Canada	1250 - 1340	bulk	120 ± 9	1054 ± 22	0.077	Malczewski et al. 2015
	Bancroft, Ontario	ca. 1150	125-250	121 ± 1	776 ± 5	0.60 ± 0.01	This study
Apatite	NA	NA	<5000	0.25 – 0.095	NA	0.5-25	Rama 1990a
	NA	NA	NA	NA	NA	0.8	
	Bancroft, Ontario	1200	<125	0.64 ± 0.01	1.08 ± 0.01	5.4 ± 0.11	This study
Hornblende	NA	NA	212-425	0.0106 ± 0.0005	NA	3.42 ± 0.38	Krishnaswami 1988
	Bancroft, Ontario	1200	<125	1.52 ± 0.01	0.308 ± 0.006	0.90 ± 0.03	This study
Quartz	Austria	NA	250-500	0.800 ± 0.03	NA	4.6 ± 0.5	Sakoda et al. 2010
	Bancroft, Ontario	1200	<125	0.0177 ± 0.0005	BDL	3.8 ± 0.46	This study

610 *Sakoda et al., 2011; Nazaroff, 1992.
611 NA: Not available.
612

This is a preprint, the final version is subject to change, of the American Mineralogist (MSA)
Cite as Authors (Year) Title. American Mineralogist, in press.
(DOI will not work until issue is live.) DOI: http://dx.doi.org/10.2138/am-2017-6017

613 Table 3. Radon emanation coefficients determined on different grain sizes at different temperatures in a suite of minerals. Uncertainties are propagated from counting statistics.

Sample	Grain size (μm)	Temperature (°C)	REC (%)	Sample	Grain size (μm)	Temperature (°C)	REC (%)	Sample	Grain size (μm)	Temperature (°C)	REC (%)
Zircon (Malawi)	125-250	25	0.37 ± 0.02	Thorite	125-250	25	0.60 ± 0.01	Hornblende	<125	25	0.90 ± 0.03
		200	0.28 ± 0.02			200	0.36 ± 0.01	Apatite			5.4 ± 0.1
		300	0.29 ± 0.02			300	0.58 ± 0.01	Augite			7.0 ± 0.2
		400	0.47 ± 0.03			400	0.58 ± 0.01	Microcline			1.28 ± 0.03
		600	0.33 ± 0.02			600	0.21 ± 0.01	Albite			0.35 ± 0.76*
		800	0.19 ± 0.03			800	0.25 ± 0.01	Quartz			3.8 ± 0.5*
	<63	25	0.77 ± 0.02	Euxenite	125-250	25	0.083 ± 0.003	Olivine			2.7 ± 0.7*
	63-125	25	0.40 ± 0.02			200	0.061 ± 0.003				
	250-500	25	0.35 ± 0.02			300	0.053 ± 0.003				
Zircon (Bancroft)	125-250	25	0.19 ± 0.01			400	0.062 ± 0.003				
		200	0.20 ± 0.01			600	0.062 ± 0.003				
		300	0.25 ± 0.01			800	0.109 ± 0.003				
		400	0.13 ± 0.01	Uraninite	125-250	25	0.177 ± 0.001				
		600	0.17 ± 0.01			200	0.102 ± 0.001				
		800	0.044 ± 0.009			300	0.263 ± 0.001				
	<63	25	0.29 ± 0.01			400	0.091 ± 0.001				
	63-125	25	0.21 ± 0.01			600	0.061 ± 0.001				
	250-500	25	0.18 ± 0.01			800	0.038 ± 0.001				
Zircon (Mud Tank)	125-250	25	0.38 ± 0.20*	Betafite	125-250	25	0.147 ± 0.002				
		200	<0.01			200	0.073 ± 0.002				
		300	<0.01			300	0.067 ± 0.002				
		400	<0.01			400	0.119 ± 0.002				
		600	<0.01			600	0.068 ± 0.002				
		800	<0.01			800	0.034 ± 0.001				
	<63	25	18.2 ± 0.4								
	63-125	25	0.72 ± 0.30								
	250-500	25	<0.01								

614 *high error is due to low radon concentration.

This is a preprint, the final version is subject to change, of the American Mineralogist (MSA)
Cite as Authors (Year) Title. American Mineralogist, in press.
(DOI will not work until issue is live.) DOI: http://dx.doi.org/10.2138/am-2017-6017

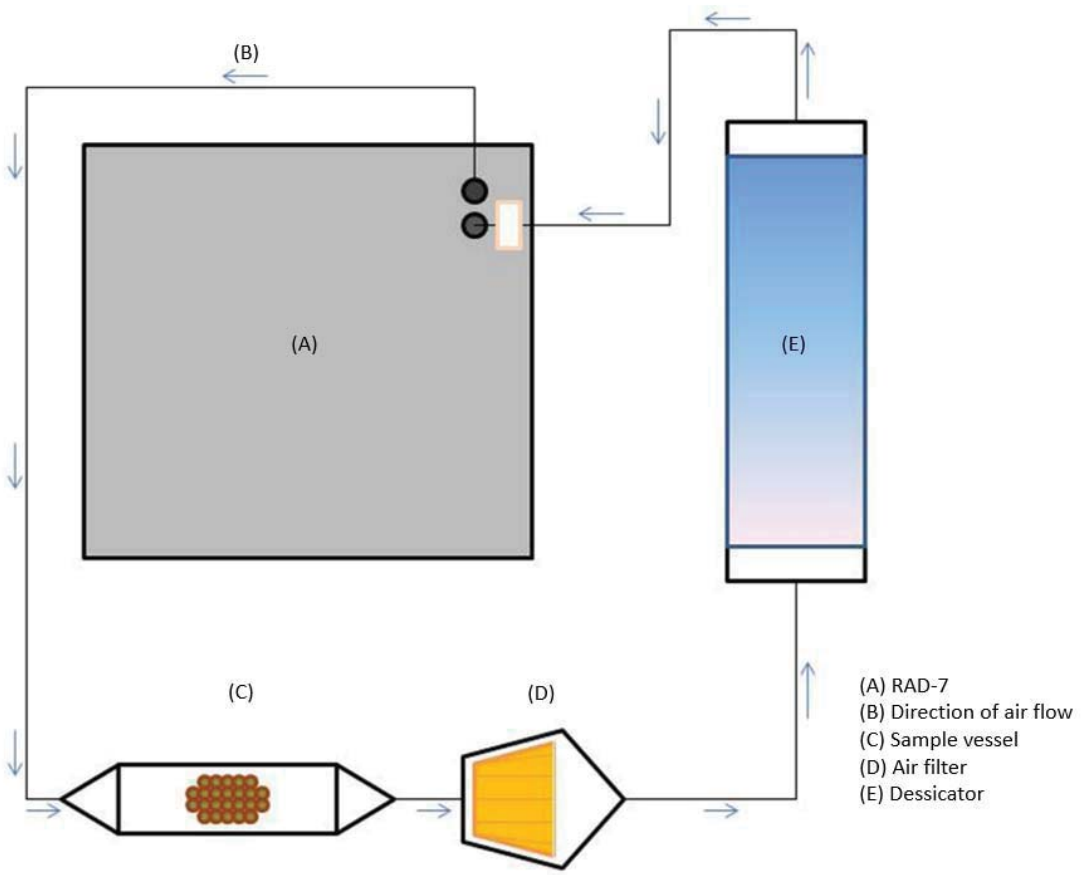

Figure 1

This is a preprint, the final version is subject to change, of the American Mineralogist (MSA)
Cite as Authors (Year) Title. American Mineralogist, in press.
(DOI will not work until issue is live.) DOI: http://dx.doi.org/10.2138/am-2017-6017

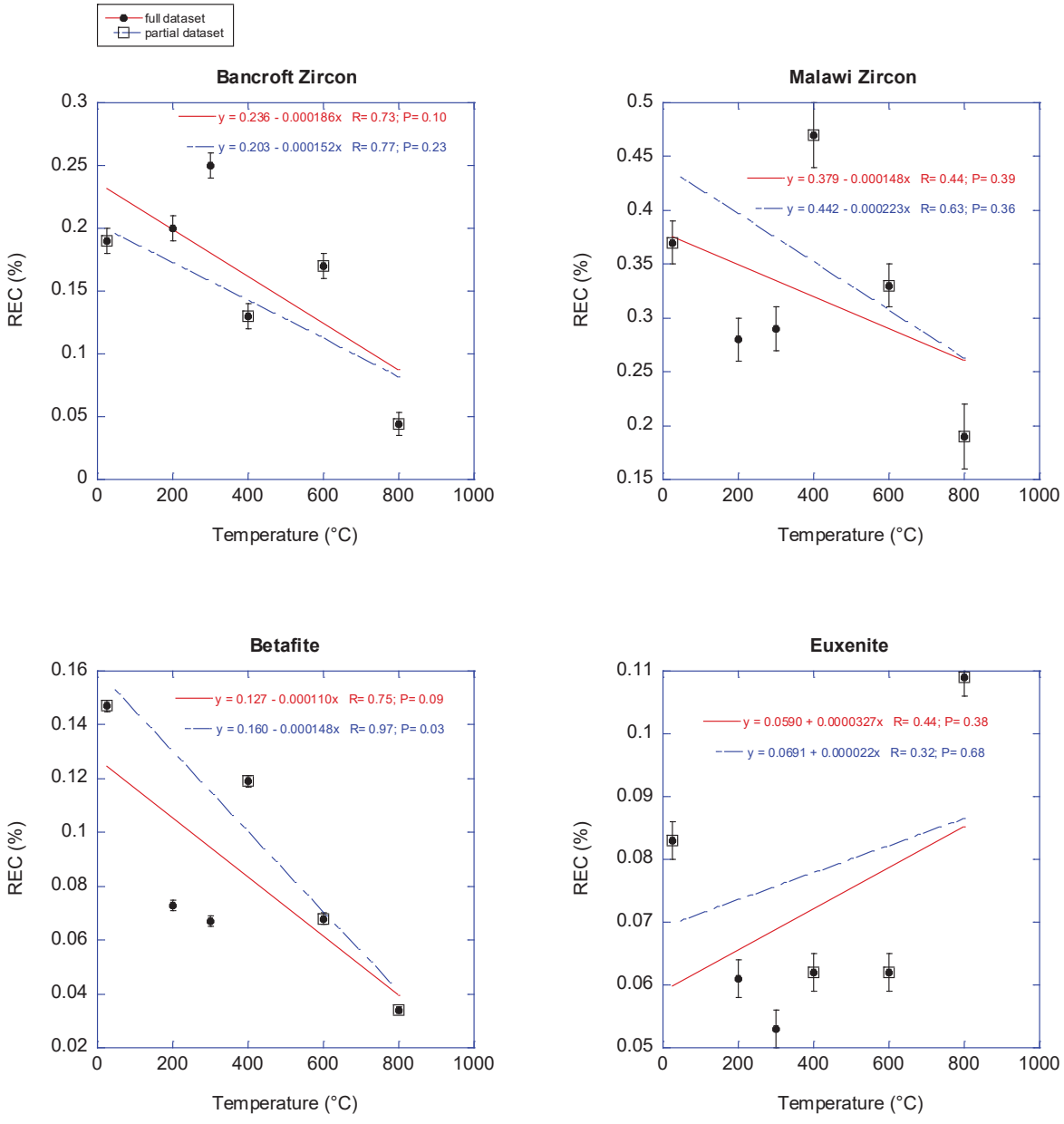

This is a preprint, the final version is subject to change, of the American Mineralogist (MSA)
Cite as Authors (Year) Title. American Mineralogist, in press.
(DOI will not work until issue is live.) DOI: http://dx.doi.org/10.2138/am-2017-6017

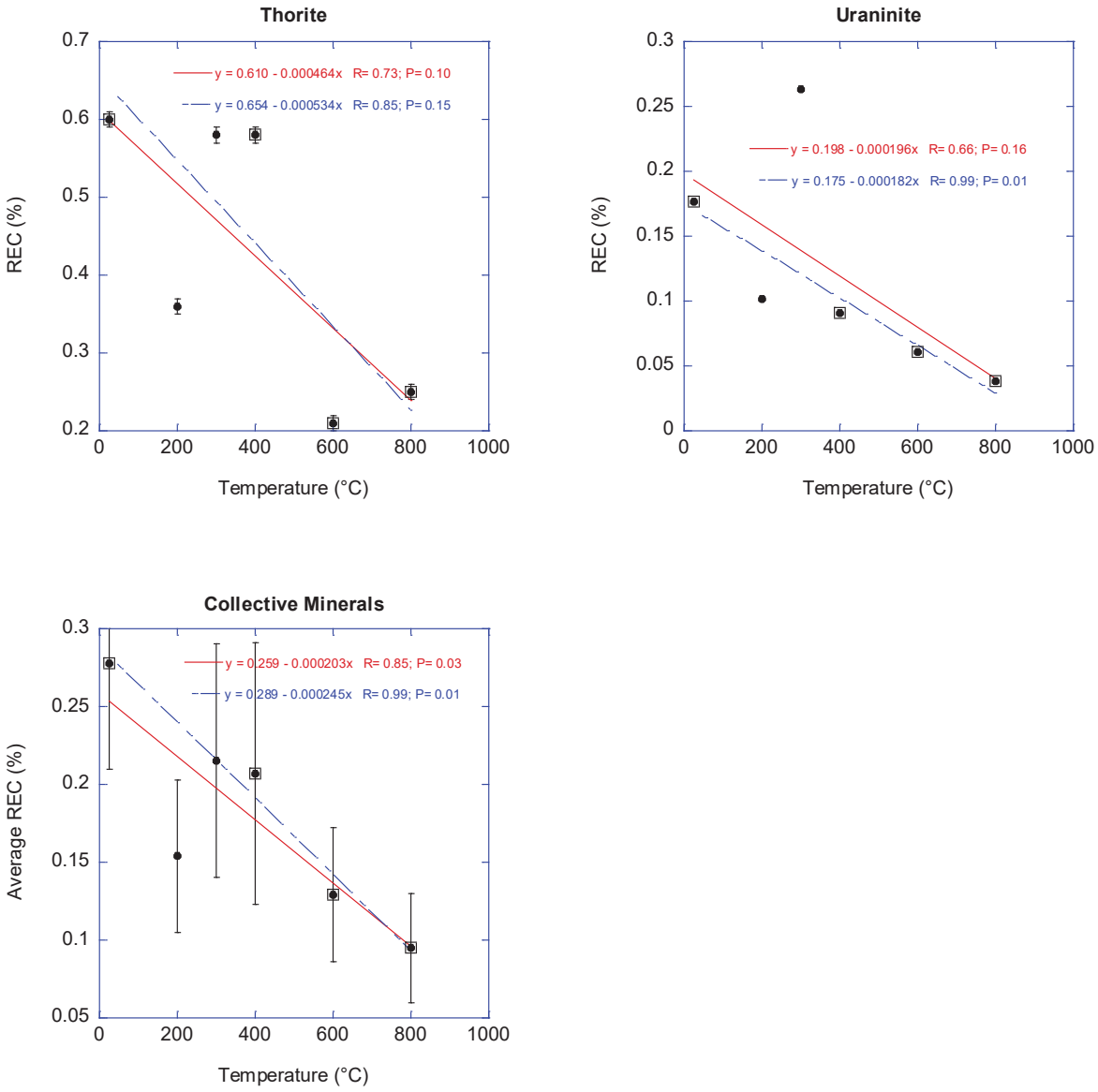

Figure 2: Radon emanation coefficient (%, average value used for plots) as a function of temperature. The linear fit is given for the full dataset as well as a partial dataset (which excludes REC values at 200° and 300°C). Error bars are included for all data points (not visible in cases when errors are smaller than the symbol size). Mud Tank zircon dataset is not included due to below detection level of radon emanation upon heating.

This is a preprint, the final version is subject to change, of the American Mineralogist (MSA)
Cite as Authors (Year) Title. American Mineralogist, in press.
(DOI will not work until issue is live.) DOI: http://dx.doi.org/10.2138/am-2017-6017

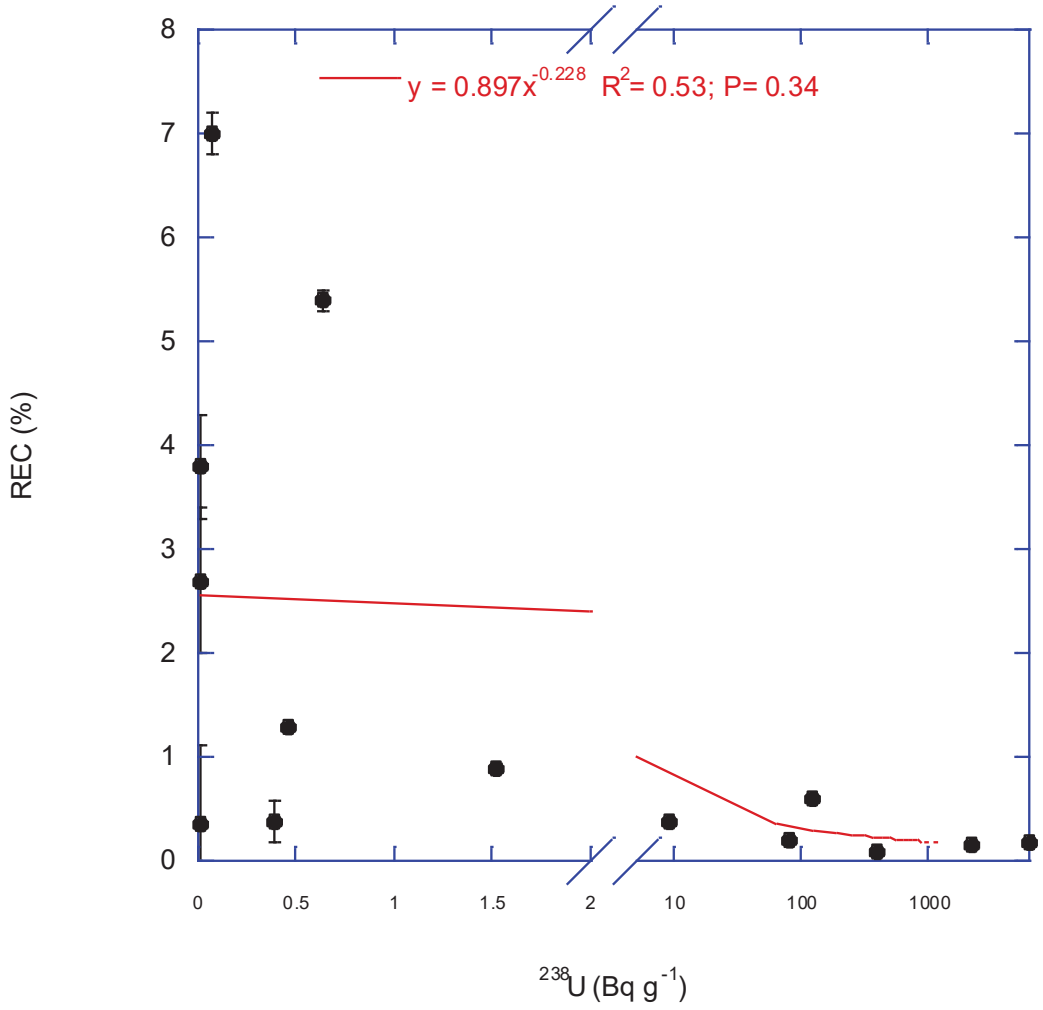

Figure 3: A plot of radon emanation coefficient as a function of ^{238}U activity for all unheated minerals. Error bars are included for all data points (not visible in cases when errors are smaller than the symbol size).

This is a preprint, the final version is subject to change, of the American Mineralogist (MSA)
Cite as Authors (Year) Title. American Mineralogist, in press.
(DOI will not work until issue is live.) DOI: http://dx.doi.org/10.2138/am-2017-6017

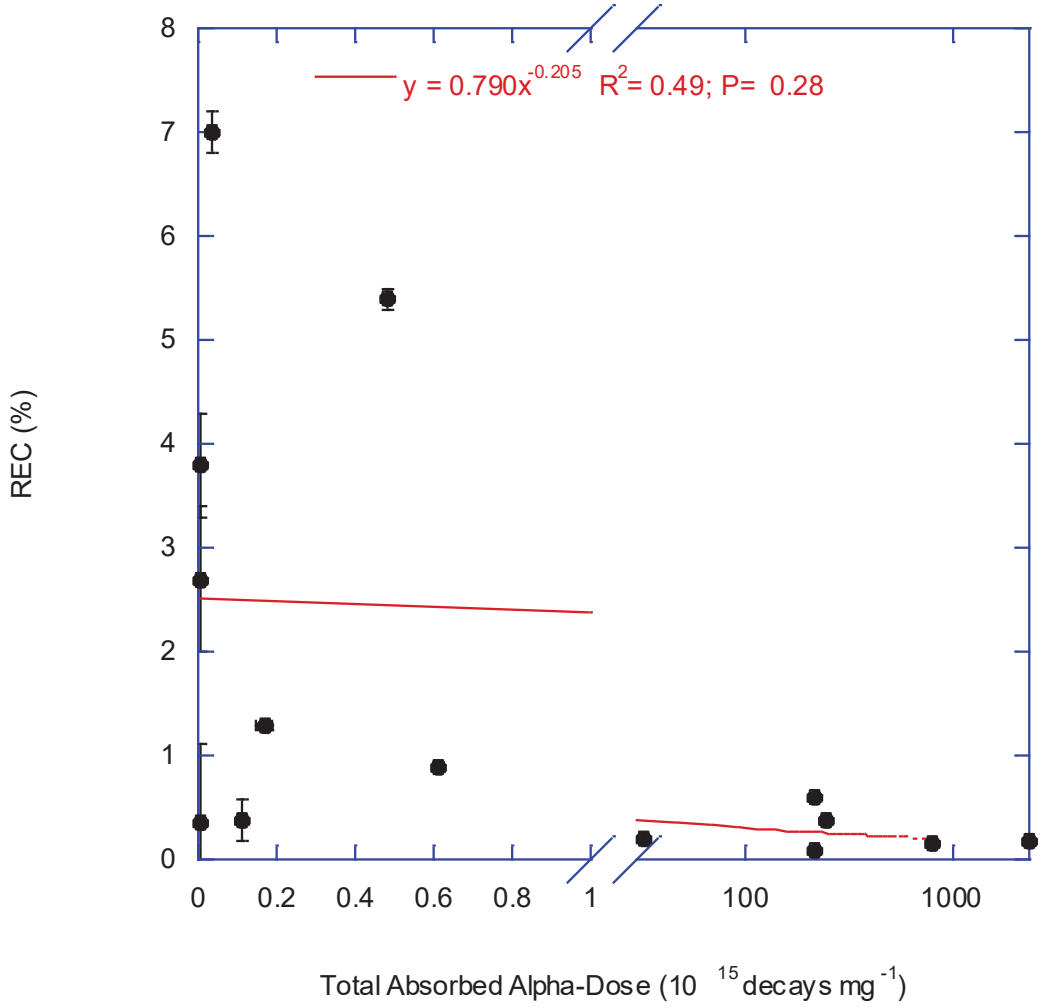

Figure 4: A plot of radon emanation coefficient versus total absorbed alpha dose for all unheated mineral samples. Error bars are included for all data points (not visible in cases when errors are smaller than the symbol size).

This is a preprint, the final version is subject to change, of the American Mineralogist (MSA)
Cite as Authors (Year) Title. American Mineralogist, in press.
(DOI will not work until issue is live.) DOI: http://dx.doi.org/10.2138/am-2017-6017

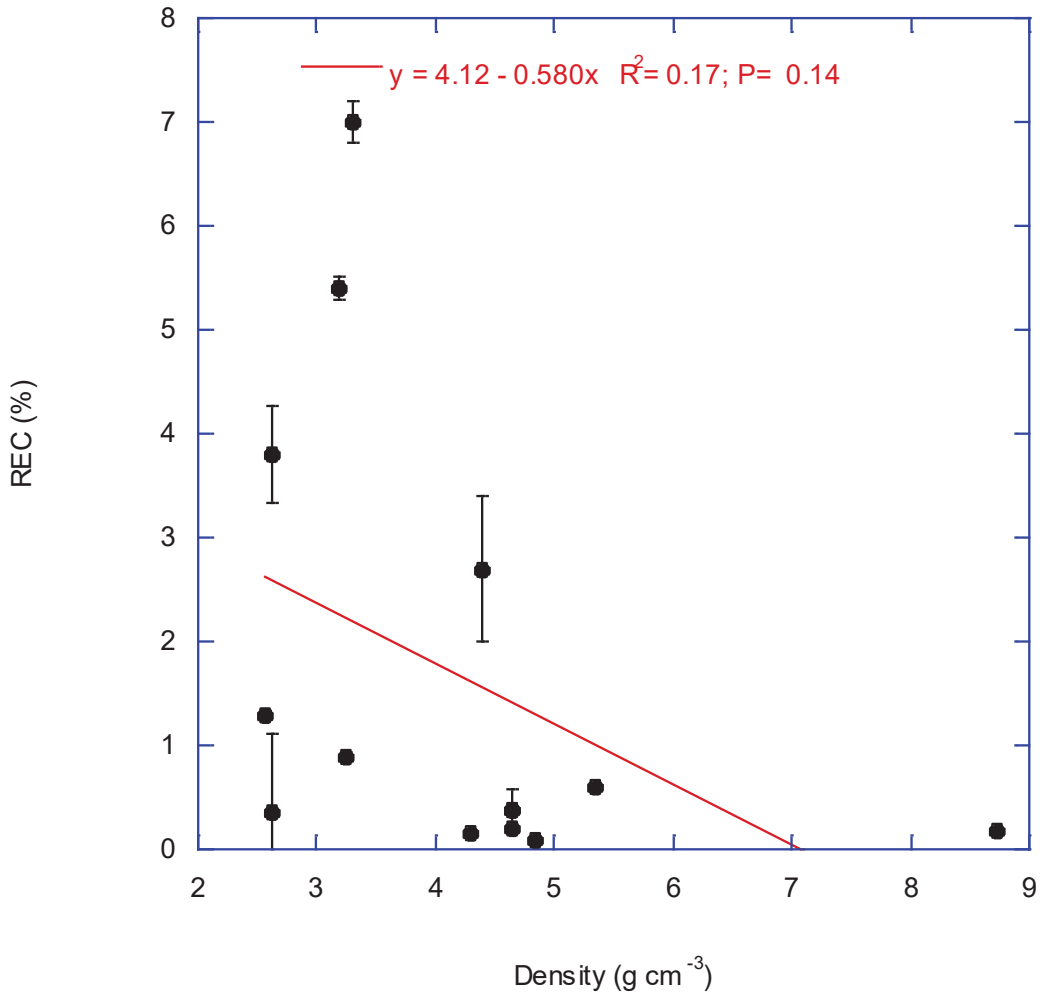

Figure 5: The radon emanation rate as a function of density for all unheated minerals of <250 µm. Error bars are included for all data points (not visible in cases when errors are smaller than the symbol size).

This is a preprint, the final version is subject to change, of the American Mineralogist (MSA)
Cite as Authors (Year) Title. American Mineralogist, in press.
(DOI will not work until issue is live.) DOI: http://dx.doi.org/10.2138/am-2017-6017

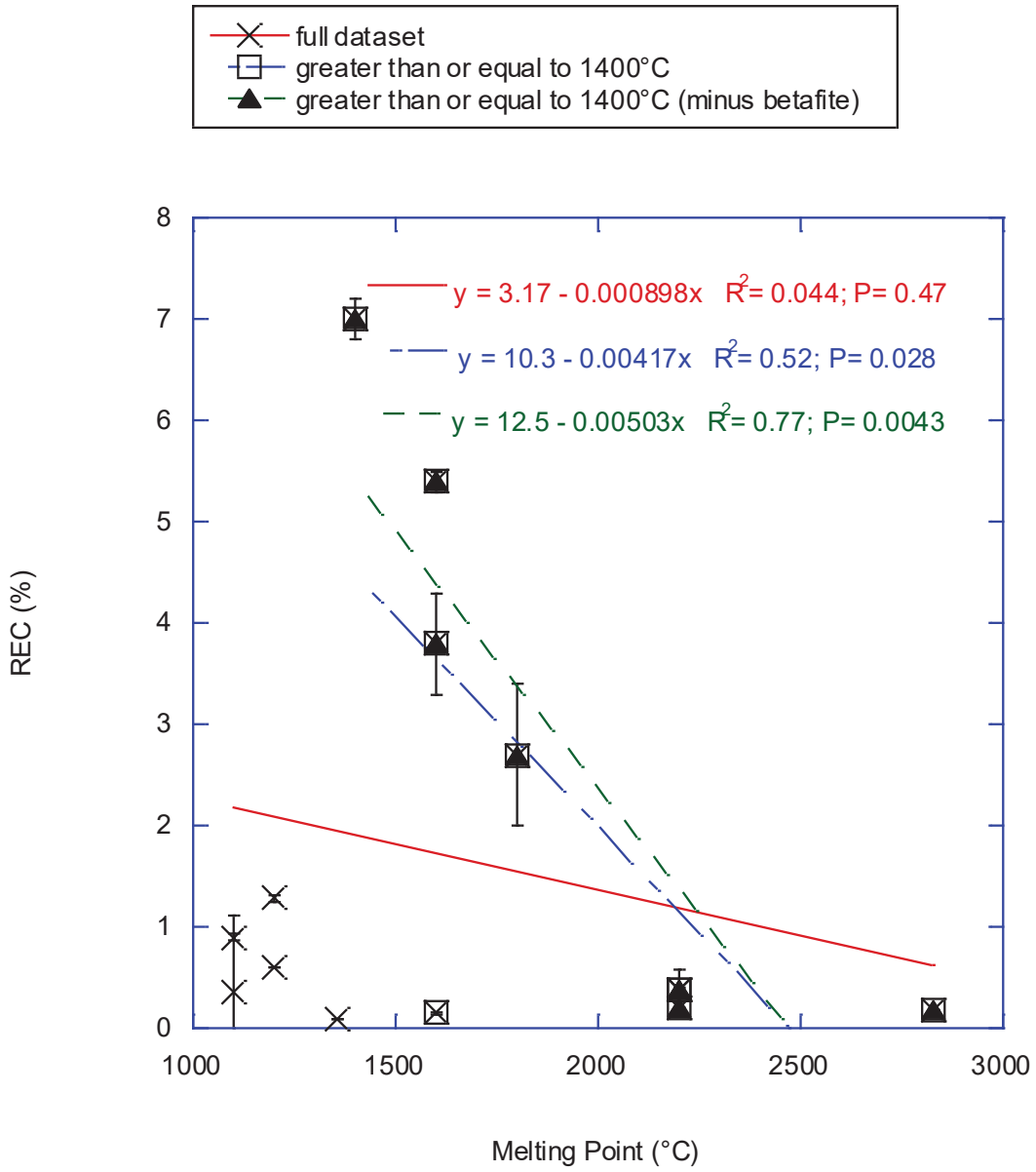

Figure 6: The radon emanation coefficient as a function of melting point (data in Table 3) for 1) all unheated minerals (red), 2) mineral samples with melting points ≥ 1400°C (blue), and 3) for minerals with melting points ≥1400°C, excluding betafite (green). There is no significant correlation for the whole sample set, but for minerals with ≥ 1400°C melting temperature, there is a significant correlation.